Nat. Hazards Earth Syst. Sci., 15, 487–504, 2015
www.nat-hazards-earth-syst-sci.net/15/487/2015/
doi:10.5194/nhess-15-487-2015

Natural Hazards and Earth System Sciences
Open Access

Future discharge drought across climate regions around the world modelled with a synthetic hydrological modelling approach forced by three general circulation models

N. Wanders[1] **and H. A. J. Van Lanen**[2]

[1]Department of Physical Geography, Utrecht University, Utrecht, the Netherlands
[2]Hydrology and Quantitative Water Management Group, Wageningen University, the Netherlands

Correspondence to: N. Wanders (n.wanders@uu.nl)

Received: 20 September 2013 – Published in Nat. Hazards Earth Syst. Sci. Discuss.: 23 December 2013
Revised: 1 January 2015 – Accepted: 24 February 2015 – Published: 10 March 2015

Abstract. Hydrological drought characteristics (drought in groundwater and streamflow) likely will change in the 21st century as a result of climate change. The magnitude and directionality of these changes and their dependency on climatology and catchment characteristics, however, is uncertain. In this study a conceptual hydrological model was forced by downscaled and bias-corrected outcome from three general circulation models for the SRES A2 emission scenario (GCM forced models), and the WATCH Forcing Data set (reference model). The threshold level method was applied to investigate drought occurrence, duration and severity. Results for the control period (1971–2000) show that the drought characteristics of each GCM forced model reasonably agree with the reference model for most of the climate types, suggesting that the climate models' results after post-processing produce realistic outcomes for global drought analyses. For the near future (2021–2050) and far future (2071–2100) the GCM forced models show a decrease in drought occurrence for all major climates around the world and increase of both average drought duration and deficit volume of the remaining drought events. The largest decrease in hydrological drought occurrence is expected in cold (D) climates where global warming results in a decreased length of the snow season and an increased precipitation. In the dry (B) climates the smallest decrease in drought occurrence is expected to occur, which probably will lead to even more severe water scarcity. However, in the extreme climate regions (desert and polar), the drought analysis for the control period showed that projections of hydrological drought characteristics are most uncertain. On a global scale the increase in hydrological drought duration and severity in multiple regions will lead to a higher impact of drought events, which should motivate water resource managers to timely anticipate the increased risk of more severe drought in groundwater and streamflow and to design pro-active measures.

1 Introduction

Droughts are caused by situations with less than normal natural water availability. They occur in all components of the hydrological cycle and occur across all climate regions throughout the globe (Wilhite, 2000; Tallaksen and Van Lanen, 2004; Mishra and Singh, 2010; Sheffield and Wood, 2011). On a global scale drought is one of the most severe natural hazards with large environmental and socio-economic impacts and more attention is require to be better prepared for the future water, food and energy security (Romm, 2011; Van Vliet et al., 2012). The recent summer droughts in Russia and Central United States (National Oceanic and Atmospheric Administration, 2012) were the most severe on record. The 2011 drought in the Horn of Africa caused large famine across Djibouti, Ethiopia, Kenya and Somalia (United Nations, 2011). In Europe almost 80 000 people died due to drought-related heat waves and forest fires, overall losses were estimated to be as high as EUR 4940 billion over the period 1998–2009 (EEA, 2010). Seneviratne et al. (2012) report that there is medium confidence that since the 1950s some regions of the world have experienced longer and more severe droughts (e.g. southern Europe and West Africa) and that droughts

will intensify in the 21st century in some seasons and areas (e.g. many European regions, parts of North America, Central America, southern Africa) as a result of climate change. Lack of long, continuous time series of observed hydrological data (e.g. Hannah et al., 2011; Stahl et al., 2012), multiple definitions and drought-generating processes (e.g. Van Loon and Van Lanen, 2012), and the incapability of models to include all these processes (e.g. Gudmundsson et al., 2012; Haddeland et al., 2011; Prudhomme et al., 2011) reduce our ability to instil strong confidence in the assessment of past and future drought across the world. High-impact large-scale droughts, like the recent droughts in Russia, United States and Africa, show the need to improve understanding of drought mechanisms on continental and global scales, which would lead to better drought adaptation and drought predictability. Improved understanding will also help to provide an improved assessment of climate change impact on drought.

Most global drought studies and near-real time drought monitoring programmes focus on meteorological drought (in particular SPI, McKee et al., 1993), since meteorological data are widely available on a global scale. Other research has focused on soil moisture droughts on the global scale (e.g. Dai et al., 2004; Sheffield and Wood, 2007; Sheffield et al., 2009; Dai, 2011; Orlowsky and Seneviratne, 2013). Global soil moisture droughts have been often examined (e.g. Dai et al., 2004; Dai, 2011; Sheffield et al., 2012) with the Palmer Drought Severity Index (PDSI Palmer, 1965), which is calculated from a simple soil water balance, with the threshold method in combination with a more comprehensive model (e.g. Sheffield and Wood, 2007; Sheffield et al., 2009) or through anomalies (e.g. Orlowsky and Seneviratne, 2013). For water resources, it is particularly relevant how meteorological and soil moisture droughts propagate into hydrological drought (e.g. Peters et al., 2003; Tallaksen et al., 2009; Van Loon and Van Lanen, 2012). At large scales, global hydrological models (GHMs) are used to produce runoff time series, which are then used for hydrological drought assessment. At the continental scale, Andreadis et al. (2005) investigated runoff drought in the United States and Prudhomme et al. (2011) studied European runoff drought. Forzieri et al. (2014) project for the A1B scenario that future drought in streamflow will increase in many European regions, except for North and Northeast Europe. Corzo Perez et al. (2011b), Van Huijgevoort et al. (2012) and Wanders et al. (2015) showed the changes in hydrological drought characteristics at the global scale. These large-scale studies investigate which characteristics (frequency, scale, duration, severity) of past hydrological drought are captured with the GHMs to explore their potential to assess future continental and global drought. Recently, the WATCH (WATer and global CHange) project concluded a comprehensive multi-model analysis (e.g. Haddeland et al., 2011) that tested GHM performance against historic low runoff (e.g. Gudmundsson et al., 2012; Stahl et al., 2012) and drought (e.g. Prudhomme et al., 2011). Corzo Perez et al. (2011b) made a first attempt to use the outcome from the WATCH model suite to assess future hydrological drought across the globe – three general circulation models (GCMs), two scenarios, multiple hydrological models. The WATCH model suite was further assessed by Van Huijgevoort et al. (2014) for some major river basins. They showed that largest uncertainty in the projections of future hydrological drought is found in the temperate climate and this uncertainty is mainly caused by the uncertainty in the GHMs. This large uncertainty in the GHMs was also found by Prudhomme et al. (2014) for the CMIP5 climate projections in the ISI-MIP project. Prudhomme et al. (2014) compared a large ensemble of GCM–GHM combinations and showed that the highest projection uncertainty could be related to the GHM runoff-generating processes – which is supported by the work of Haddeland et al. (2011) and Hagemann et al. (2013). It was found by Alderlieste et al. (2014) that the change in the projected characteristics of future drought is larger (climate signal) than the uncertainty in the GCM–GHM combinations. Moreover, Orlowsky and Seneviratne (2013) states that the GHM impact on soil moisture projection uncertainty is most dominant for the first half of the 21st century, while in the second half the GCM uncertainty increases and has a bigger impact on the projection uncertainty.

A detailed impact assessment on the importance of climate and catchment structure on drought occurrence is complicated since GHMs have a complex model structure with a large number of internal and external feedbacks mechanisms. Moreover, the impact of GHMs on future drought projections is significant (e.g. Haddeland et al., 2011; Van Huijgevoort et al., 2014; Prudhomme et al., 2014), which makes a detailed impact assessment of the importance of climate and catchment structure even more complicated. To investigate the relative importance of climate and catchment structure on hydrological drought, Van Lanen et al. (2013) used a synthetic hydrological modelling approach to study the effects of these factors on hydrological drought characteristics on a global scale. The approach involved a conceptual hydrological model that was applied to a set of possible realizations of catchment characteristics (synthetic catchments) in combination with precipitation and evapotranspiration data from different climates around the globe. With this set-up Van Lanen et al. (2013) examined the relative importance of the physical catchment structure and meteorological forcing data (i.e. precipitation and evapotranspiration). They conclude that the physical catchment structure (i.e. the responsiveness of the groundwater system and soil type) has a similar impact on drought characteristics as climatology. However, the climate impact on future hydrological drought across the world is largely unknown and difficult to study (Corzo Perez et al., 2011b).

The advantage of the synthetic approach used by Van Lanen et al. (2013) is that it makes it possible to single out the impacting factors of future hydrological drought. Because a

single model set-up and parametrization was used for all locations in the world, this makes it possible to isolate the impact of climate. The advantage of the GCM–GHM combinations is that they provide the full uncertainty range of the projections, due to the large number of combinations. On the other hand, it is difficult to obtain process-based knowledge from these large ensembles. When compared to the multi-GHM simulations, the synthetic approach is not impacted by the local parametrization nor by conditions like local water abstractions or the influence of reservoirs on river flow, in the case of non-natural conditions. These processes are included in most of the GHM simulations and have a significant impact on future hydrological drought (Wanders and Wada, 2014). In a synthetic approach the influences are identical throughout the world, which will provide more knowledge on the hydrological processes that impact drought characteristics. This makes the synthetic approach an appropriate way to isolate impacting factors and processes on hydrological drought.

The objective of this study is to examine the impact of climate change on hydrological drought at a global scale. In that sense, it adds to the few existing impact studies (e.g. Prudhomme et al., 2014). However, we add to these studies by elaborating the projected hydrological drought in more depth: (i) distribution of different drought characteristics over major climates (e.g. similarities), and (ii) assessment of deficit volumes (e.g. distribution of the annual total cumulative deficit volume over the year per major climate). This has been done for different time windows (1971–2000; 2021–2050; 2071–2100). Following the synthetic approach of Van Lanen et al. (2013) a conceptual hydrological model was used to model groundwater discharge time series at randomly selected locations in various climate regions around the world. Three GCMs provided model forcing data to the hydrological model and simulated droughts were compared against those derived from quasi-observational data (WATCH) forced model over the period 1971–2000 to explore uncertainty due to GCM forcing. Thereafter the effect of climate change was studied by the inter-comparison of modelled groundwater discharge time series and associated drought characteristics against the control period (1971–2000) for all GCM scenarios and the periods 2020–2050 and 2070–2100. The results allow a discussion on the projected impact of climate change on hydrological drought characteristics, including uncertainty, which, in addition to impacts on meteorological and soil water drought characteristics, provide key information for planning of future water resources.

2 Forcing data

2.1 WATCH Forcing Data

The WATCH Forcing Data (WFD) consist of time series of meteorological variables (e.g. rainfall, snowfall, temperature, wind speed) and are a product of the EU-FP6 project WATCH (WATer and global CHange). The WFD are derived from bias-corrected ECMWF ERA-40 reanalysis data (Uppala et al., 2005), which have a sub-daily, 1° resolution. For the WFD these data have been downscaled to 0.5° and temperature and specific humidity were bias corrected for elevation difference between the ERA-40 grid and WFD grid (Weedon et al., 2010, 2011). Bias corrections were applied to the daily temperature cycle and average temperature values using the CRU 2.0 data (Mitchell and Jones, 2005) and to the number of "wet" days using the CRU data, while monthly rainfall and snowfall totals were corrected with the GPCCv4 data set (Schneider et al., 2008). The CRU grid was used for the projection of the WFD resulting in a total of 67,420 land points at $0.5° \times 0.5°$ resolution. The WFD for the period 1971–2000 have been used as a reference forcing data set in this study. The WFD were successfully used in multiple hydrological studies (e.g. Corzo Perez et al., 2011a; Haddeland et al., 2011; Harding et al., 2011; Prudhomme et al., 2011; Gudmundsson et al., 2012; Stahl et al., 2012; Van Vliet et al., 2012; Van Huijgevoort et al., 2013; Van Loon et al., 2014). In this study the WFD were used to identify the reference hydrological situation for every selected location, with the synthetic hydrological modelling approach.

2.2 General circulation models

In this study the output from three coupled atmosphere–ocean GCMs for the SRES A2 scenario (Nakićenović and Swart, 2000) has been used. The SRES A2 scenario includes extensive emission of carbon dioxide and slow adaptation by the global population, leading to severe changes in future climatology. Through the EU-WATCH project, simulation outcome from three GCMs was available on a global scale. The GCMs included are ECHAM5 (Roeckner et al., 2003; Jungclaus et al., 2006), CNRM3 (Royer et al., 2002; Salas-Mélia, 2002) and IPSL (Hourdin et al., 2006; Madec et al., 1998; Fichefet and Maqueda, 1997; Goosse and Fichefet, 1999). Each GCM provides meteorological forcing for the period 1960–2100. We used the period 1971–2000 as control period. The same procedure as for the WFD was applied in WATCH to downscale each GCM to the higher resolution 0.5° grid of the WFD. The WFD were used to determine the bias correction required for rainfall, snowfall, minimum, mean and maximum air temperature for the control period. The procedure is described in more detail by Piani et al. (2010a, b), Chen et al. (2011), and Haerter et al. (2011). More detailed information on the GCMs can be found in Table 1. The data from the GCMs were used as meteorological input data for the synthetic hydrological modelling approach to produce groundwater discharge time series and associated drought characteristics for: (i) the control period (1971–2000), and (ii) the periods 2021–2050 and 2071–2100 to intercompare obtained drought characteristics against those derived from the reference model (1971–2000).

Table 1. Three IPCC AR4 GCMs and their properties.

Centre	GCM	Horizontal res.	Vertical res.
MPI	ECHAM5/MPIOM T63	$\approx 1.9° \approx 200$ km	31 layers
CNRM	CNRM-CM3 T42	$\approx 2.8° \approx 300$ km	45 layers
IPSL	IPSL-CM4	$3.75° \times 2.5° \approx 300$ km	19 layers

The advantages of this mini-ensemble is that the bias correction was performed by experts in the field both for the control period (Piani et al., 2010a, b; Haerter et al., 2011) using the WFD data set (Weedon et al., 2010, 2011) to correct the models and for the future (Hagemann et al., 2011; Chen et al., 2011). This resulted in consistent downscaled and bias-corrected GCM data for 1963–2100. The period 1963–1970 was used to initialize the hydrological model and make sure that the groundwater discharge simulations were no longer influenced by the initial conditions. Although this mini-ensemble most likely under-samples the climate variability, the advantage of having a long initialization period and a validated bias correction is deemed more important.

3 Model framework

3.1 Model description

The conceptual hydrological model is a lumped conceptual hydrological model, which consists of reservoirs for snow cover, soil moisture and groundwater (Fig. 1). The model concept is a simplified representation of the natural system that simulates daily fluxes and state variables. The conceptual hydrological model generates time series of potential realizations for soil moisture storage and groundwater discharge without use of specific local catchment information apart from meteorological forcing (synthetic catchments). The simulations do not claim to provide actual site-specific soil moisture storage and groundwater discharge, but rather give a possible realization of these variables given the local meteorological data (e.g. Van Lanen et al., 2013; Van Loon et al., 2014). The water balance of the modelled soil moisture is given by

$$\mathrm{SS}(t) = \mathrm{SS}(t-1) + (P_{\mathrm{ra}}(t) + Q_{\mathrm{sn}}(t) - E_{\mathrm{act}}(t) - Q_{\mathrm{s}}(t)) \cdot \Delta t, \quad (1)$$

where SS is the soil moisture storage (mm), P_{ra} the rainfall (mm d^{-1}), Q_{sn} the snowmelt (mm d^{-1}), E_{act} the actual evapotranspiration (mm d^{-1}), $Q_{\mathrm{s}}(t)$ is groundwater recharge generated by percolation through the unsaturated zone (mm d^{-1}) and Δt the time step of the model, which is 1 day for all simulations. The model is forced with daily temperature, precipitation and potential evapotranspiration to enable snow accumulation, soil moisture, actual evapotranspiration and discharge simulations. Estimates of daily evapotranspiration are calculated using the Penman–Monteith reference evapotranspiration (McMahon et al., 2013). The potential evapotranspiration was calculated from daily temperature (minimum, mean, maximum), air pressure, humidity and wind speed (Allen et al., 2006). The daily mean temperature was also used in the snow module for snow accumulation and melt, following the widely accepted approach of the HBV model (Seibert, 2002). Precipitation is simulated as snow when air temperature is below a pre-defined threshold, snowmelt only occurs above the threshold temperature and is simulated with the degree-days approach (Clyde, 1931; Collins, 1934). The snow water balance of the snow module is given by

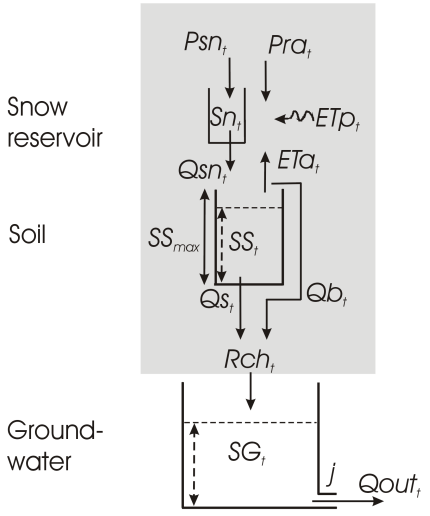

Figure 1. Model set-up of the conceptual hydrological model used in this study. The model consists of three partitions, Snow, Soil and Groundwater. P_{sn} snowfall, P_{ra} rainfall, $\mathrm{ET_p}$ potential evapotranspiration, $\mathrm{ET_a}$ actual evapotranspiration, S_{n} snow storage, SS soil storage, $\mathrm{SS_{max}}$ maximum soil storage, Q_{sn} snowmelt, Q_{s} recharge to the groundwater from the unsaturated zone, Q_{b} bypass flow, R_{ch} total recharge to groundwater, SG groundwater storage, j groundwater response parameter, Q_{out} groundwater discharge and t is the time index.

$$\mathrm{Sn}(t) = \mathrm{Sn}(t-1) + (P_{\mathrm{sn}}(t) - Q_{\mathrm{sn}}(t)) \cdot \Delta t, \quad (2)$$

where Sn is the snow storage (mm) and P_{sn} is snowfall (mm d^{-1}). The groundwater recharge (mm d^{-1}) is given by

$$R_{\mathrm{ch}}(t) = Q_{\mathrm{s}}(t) + Q_{\mathrm{b}}(t), \quad (3)$$

where $Q_{\mathrm{s}}(t)$ is recharge generated by unsaturated zone (mm d^{-1}) and $Q_{\mathrm{b}}(t)$ is recharge generated by bypass in the unsaturated zone (mm d^{-1}). The percolation through the un-

saturated zone is given by

$$Q_s(t) = (SS(t) - SS_{FC}) \cdot \Delta t \text{ if } SS(t) \geq SS_{FC}$$
$$Q_s(t) = \left(\left(\frac{SS(t) - SS_{CR}}{SS_{FC} - SS_{CR}} \right)^b k_{FC} \right) \cdot \Delta t \quad (4)$$
$$\text{if } SS_{CR} \leq SS(t) \leq SS_{FC}$$
$$Q_s(t) = 0 \text{ if } SS(t) \leq SS_{CR},$$

where $SS(t)$ (mm) is the soil moisture content at time t (in d), b is a shape parameter derived from the soil retention curve (–), k_{FC} is the unsaturated hydraulic conductivity at field capacity (mm d^{-1}), SS_{CR} (95.2 mm) and SS_{FC} (168.9 mm) are the critical and field capacity soil moisture content, respectively. The bypass to the groundwater $Q_b(t)$ is 50 % of the rainfall above 2 mm, when the soil is below SS_{CR} to simulate flow through the macropores of the unsaturated zone. A soil with an intermediate soil moisture supply capacity was selected to simulate the response of the unsaturated zone (Van Lanen et al., 2013). This soil has a total supply capacity of 125.4 mm (from SS_{FC} to wilting point, SS_{WP} is 43.5 mm) where about 75 mm (between SS_{FC} and SS_{CC}) is readily available for evapotranspiration. Below SS_{CC} the evapotranspiration is linearly reduced to 0.0 mm d^{-1} at SS_{WP}. The water balance of the groundwater system is given by

$$SG(t) = SG(t-1) + (R_{ch}(t) - Q_{out}(t)) \cdot \Delta t, \quad (5)$$

where SG is the groundwater storage (mm) and Q_{out} is the groundwater discharge (mm d^{-1}). The Q_{out} is calculated with the De Zeeuw–Hellinga approach (Kraijenhof van de Leur, 1962; Ritzema, 1994):

$$Q_{out}(t) = Q_{out}(t-1) \cdot e^{\frac{-1}{j}} + R_{ch}(t) \cdot \left(1 - e^{\frac{-1}{j}}\right) \quad (6)$$

where j is the groundwater response parameter (in d), which can be derived from data on the aquifer transmissivity, storativity and the distance between rivers. The j-value in this study was fixed to 250 d, which corresponds to an intermediate-responding groundwater system. The groundwater discharge is hereafter called discharge ($Q = Q_{out}$). The ability of the conceptual model to reproduce observed streamflow was demonstrated by Tijdeman et al. (2012). The conceptual model was evaluated against observed drought characteristics of four contrasting catchments in Europe. It was shown that the model is capable to correctly simulate hydrological drought characteristics. The Nash–Sutcliffe (NS, Nash and Sutcliffe, 1970) for the selected catchments was between 0.35 and 0.75, with an improved performance for the low-flow conditions (NS 0.35–0.85). For a more detailed description of the conceptual hydrological modelling, sensitivity analysis or the validation results, the reader is referred to Tijdeman et al. (2012), Van Lanen et al. (2013) and Van Loon et al. (2014).

3.2 Drought identification

Hydrological drought characteristics (e.g. drought duration and deficit volume) were derived from simulated time series of daily groundwater discharge (Q) using the threshold level approach (Yevjevich, 1967; Tallaksen et al., 1997; Hisdal et al., 2004). In this study the Q_{80} (mm d^{-1}) was derived from the flow duration curve, where the Q_{80} is the threshold which is equalled or exceeded for 80 % of the time. The Q_{80} has been used in multiple studies where drought is studied (e.g. Fleig et al., 2006; Parry et al., 2010). A monthly threshold was applied, where the Q_{80} is derived for every month of the year in the control period. With a moving average window of 30 days the threshold was smoothed, resulting in the variable monthly threshold used for this study (Van Loon and Van Lanen, 2012). The Q_{80} obtained from the reference period was also used for the future period to enable drought identification in the period 2000–2100, relative to 1971–2000. The drought state is given by

$$Ds(t) = 1 \text{ for } Q(t) < Q_{80}(t)$$
$$0 \text{ for } Q(t) \geq Q_{80}(t), \quad (7)$$

where $Ds(t)$ is a binary variable indicating whether a location is in drought at time t. The drought duration for each event was calculated with

$$Dur_i = \sum_{t=S_i}^{L_i} Ds(t), \quad (8)$$

where Dur_i is the drought duration (d) of event i, S_i the first time step of an event i and L_i the last time step of the event. The percentage drought per year (PDY) was used in this study as a measure of drought occurrence that enables a comparison between the simulated groundwater discharge time series of different time periods (e.g. 2021–2050 relative to 1971–2000). The PDY was calculated by

$$PDY = \frac{\sum_{t=1}^{T} Ds(t) \cdot 365}{T}, \quad (9)$$

where PDY is the fraction of the total simulation period that a location is in drought (d yr^{-1}) and T is the total number of time steps. Please note that PDY = 73 d yr^{-1} for the control period 1971–2000 by definition. The deficit volume was defined by

$$Def(t) = Q_{80}(t) - Q(t) \quad \text{for } Ds(t) = 1$$
$$0 \quad \text{for } Ds(t) = 0, \quad (10)$$

where $Def(t)$ is the daily deficit volume of drought i (mm). The total drought deficit volume for each drought event was calculated with

$$Def_i = \sum_{t=S_i}^{L_i} Def(t), \quad (11)$$

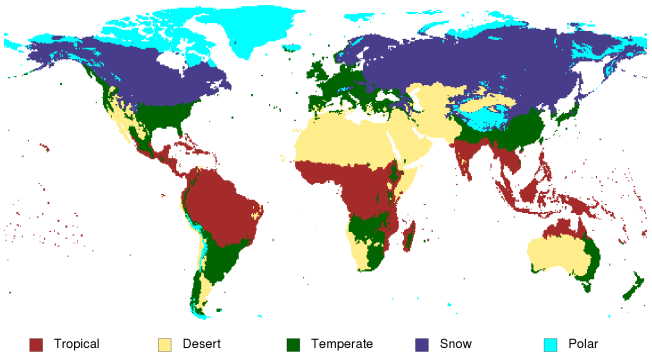

Figure 2. The Köppen–Geiger climate classification, based on the climatology of the WATCH Forcing Data (1958–2001).

where Def_i is the total deficit volume of the drought event i (mm). The deficit volume is the cumulative deviation of the discharge from the threshold over the duration of a drought event. Furthermore, the standardized deficit volume (in d) was obtained with

$$\mathrm{StDef}_i = \frac{\mathrm{Def}_i}{\overline{Q}}, \tag{12}$$

where StDef_i is the deficit volume of event i [d] divided by $\overline{Q}$, the mean yearly discharge (mm d^{-1}). StDef_i was introduced to enable a comparison across the globe between locations with different flow magnitudes. Since the deficit volume (Def_i) is highly correlated to the discharge, the obtained StDef provides the drought severity relative to the local hydrological situation. The StDef can be interpreted as the number of days that the mean yearly discharge is missing. The drought duration and standardized deficit volume are hereafter referred to as the duration and deficit volume. If the Q_{80} equals 0 mm d^{-1} for more than 20 % of the time, no drought characteristics were calculated since by definition a drought will not occur (Eq. 7). These locations were excluded from the analysis, since frequent zero-discharge situations are part of the local climate (i.e. aridity) and are not a situation with below-normal water availability. When a drought is already present at the beginning of a simulation period or still present at the end no valid average characteristics could be obtained and therefore the drought event was excluded from the analysis to avoid including incomplete drought events in the statistics.

3.3 Similarity Index

The similarity index (SI) was introduced as a measure to examine changes in drought characteristics (Van Lanen et al., 2013). Bivariate probability distributions (Wand and Jones, 1995) were used to find relations between drought duration (Eq. 8) and deficit volume (Eq. 12). The bivariate probability distributions were compared for different time periods and their joint occurrence was evaluated with the SI. The area of the 90 % of the bivariate probability distribution field was calculated and used for further evaluation. Both low and high extreme values of Dur_i and Def_i were excluded, since the focus of this study is not on changes in the most extreme drought conditions. The SI quantifies the degree of overlap (%) between two 90 % Dur–StDef probability fields as follows:

$$\mathrm{SI} = \frac{\mathrm{R1|R2}}{\mathrm{R1}} \cdot 100$$

$$\mathrm{R1} = \sum_{x=1}^{m}\sum_{Y=1}^{n} \mathbf{MR1}(m,n) \;\text{ if }\; \mathbf{MR1}(m,n) = 1 \tag{13}$$

$$\mathrm{R1|R2} = \sum_{x=1}^{m}\sum_{Y=1}^{n} \mathbf{MR1}(m,n) \;\text{ if }\; \mathbf{MR1}(m,n) = 1 \;\text{ and }\; \mathbf{MR2}(m,n) = 1,$$

where R1 is the 90 % Dur–StDef probability field of realization of period 1 (e.g. 1971–2000), R1 | R2 is the coinciding 90 % Dur–StDef probability fields of realizations of period 1 and 2 (e.g. 1971–2000 and 2021–2050, respectively), and m and n indicate probable realizations of Dur_i and Def_i. **MR1** and **MR2** are matrices, **MR1** contains the conditional probabilities of realization of period 1, and **MR2** the field of realization of period 2. $\mathbf{MR1}(m,n)$ and $\mathbf{MR2}(m,n)$ are binary quantities where 1 equals a value within, and 0 a value outside the 90 % Dur–StDef probability field of realizations 1 and 2, respectively. In this study $m \cdot n$ was set at $150 \cdot 150$ and physical limits of Dur and StDef were fixed to 1296 and 256 d, respectively. By definition the SI can range between 0 % (no joint occurrence) and 100 % (complete joint occurrence). For a more detailed description of the SI the reader is referred to Van Lanen et al. (2013).

3.4 Selection of evaluation locations

For a global evaluation of the change in drought duration and deficit volume as a result of climate change, locations (i.e. WATCH cells) were randomly selected around the world. The Köppen–Geiger climate classification (Köppen, 1900; Geiger, 1954, 1961) was used to ensure that sufficient locations were selected in all different major climate regions. The five climate types distinguished in this study are: Equatorial (A), Arid (B), Warm temperate (C), Snow (D) and Polar climates (E). The global map with Köppen-Geiger climate classification was recalculated based on the WFD, to obtain correct positioning of climate regions (Fig. 2). Van Lanen et al. (2013) found that 1495 locations were sufficient to adequately include world's climates and were also used for this study (21 locations were excluded due to high number of no-flow conditions). They show that at least 30 randomly selected locations are required per major climate region to obtain reliable general drought characteristics. The selected locations were distributed over the climate types A, B, C, D and E as follows: 16, 21, 16, 34 and 13 %, reflecting differences in area of major climate regions.

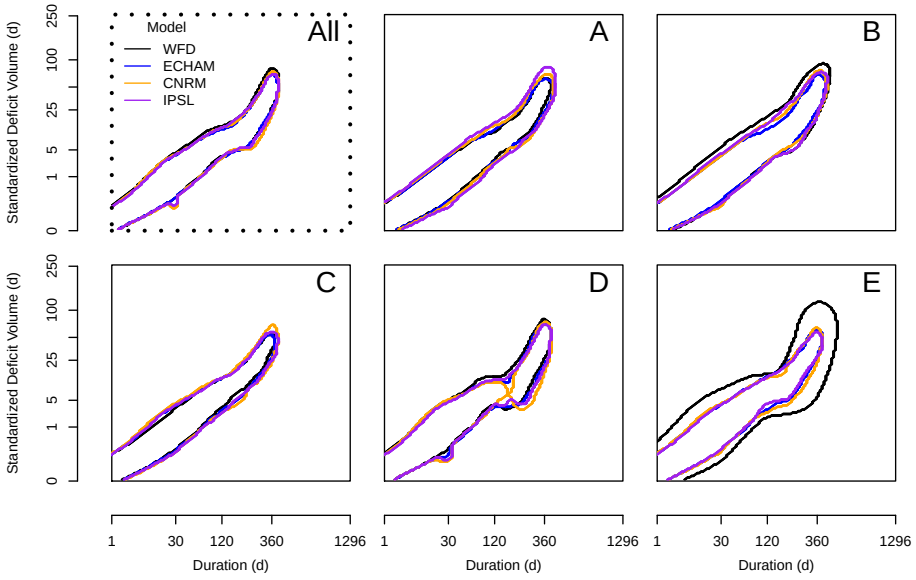

Figure 3. Bivariate probability functions for two hydrological drought characteristics (duration and standardized deficit volume) for all climate types (All) and individual major climate types, Equatorial (A), Arid (B), Warm temperate (C), Snow (D) and Polar climates (E) obtained from simulations of the conceptual hydrological model, using meteorological forcing by the WATCH Forcing Data (WFD, reference) and GCMs: ECHAM, CNRM and IPSL.

3.5 Impact assessment of climate change

To examine the impact of climate change on characteristics of groundwater discharge droughts, the synthetic hydrological modelling approach was used and forced with meteorological data from three GCMs (GCM forced) over the period 1960–2100 and the WFD over the period 1960–2000 (reference model). This period was divided into three evaluation periods, namely 1971–2000, 2021–2050, 2071–2100. An 11-year warm-up period (1960–1970) was applied for the hydrological model to remove biases resulting from the initial conditions. The monthly Q_{80} was derived over the period 1971–2000 for each simulation separately to determine the simulation-dependent variable threshold (Sect. 3.2). The 1971–2000 threshold was applied to the two other future periods (for the GCM forced simulation), to enable calculation of the drought characteristics (D and StDef, Eqs. 8 and 12), and to determine the effect of climate change relative to the period 1971–2000. The effect of climate changes on drought duration and deficit volume was studied for all different major climate regions. The groundwater discharge drought characteristics of each GCM forced hydrological model simulation over the control period (1971–2000) were compared against the characteristics derived from the model forced with the WFD reference model for the same period to explore uncertainty due to GCM forcing. Ideally, there should be only minor differences in drought characteristics between the characteristics derived from groundwater discharge simulated with the GCM forcing and the simulation with the WFD, since the control periods of each GCM are bias corrected to match the WFD (Piani et al., 2010a, b; Haerter et al., 2011; Chen et al., 2011; Hagemann et al., 2011). The changes in future drought characteristics were evaluated for the period 2021–2050 and 2071–2100 by comparing against the control period (1971–2000) of each GCM forced hydrological model simulation. For the evaluation the SI was calculated for all major climate types and used to determine the changes in drought duration and deficit volume as a result of a changing climate. For the seasonal analysis of changes in drought deficit volumes, the season for the location at the Southern Hemisphere has been transposed to match the Northern Hemisphere climatology.

4 Results

4.1 Control period

Hydrological droughts derived from groundwater discharge time series that were simulated with the synthetic hydrological modelling approach using re-analysis data (WFD) as meteorological forcing (reference model) were the benchmark in this study. The hydrological drought characteristics were intercompared for the control period from 1971–2000 with those obtained from the same hydrological model that was forced with downscaled and bias-corrected outcome from three GCM forced models.

The bivariate density distributions obtained for the control period for all three GCM forced models show large similarity with the reference model for all climate types (Fig. 3). However, some deviations occur for the polar (E)

Table 2. Similarity index (SI) between the reference model with meteorological forcing from the WATCH Forcing Data and models with meteorological forcing from three GCMs (ECHAM, CNRM, IPSL) for the control period (1971–2000). SI is given for all major climates, Equatorial (A), Arid (B), Warm temperate (C), Snow (D) and Polar climates (E), and for averaged over all climates.

	WFD					
	A	B	C	D	E	All
ECHAM	100	75	99	92	67	91
CNRM	100	82	100	87	73	94
IPSL	100	85	98	90	65	93

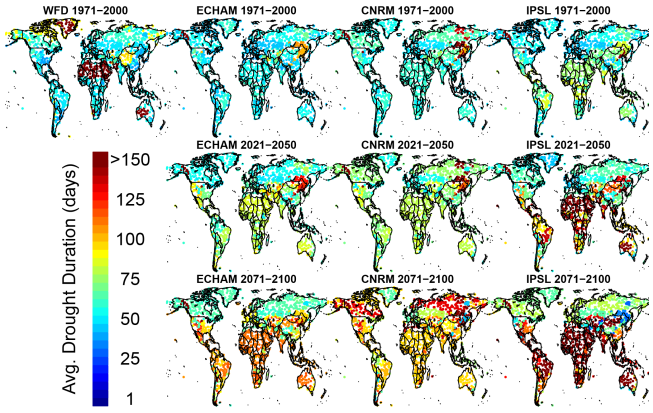

Figure 4. Spatial distribution of average hydrological drought duration for different time periods, obtained from simulations of the conceptual hydrological model, using meteorological forcing by the WATCH Forcing Data (WFD) and three GCMs: ECHAM, CNRM and IPSL.

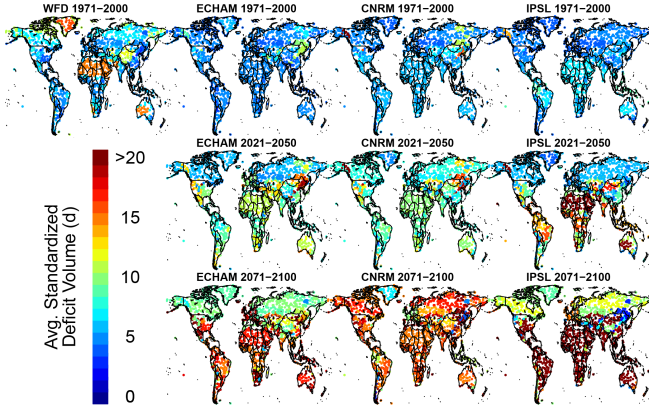

Figure 5. Spatial distribution of average standardized deficit volume for different time periods, obtained from simulations of the conceptual hydrological model, using meteorological forcing by the WATCH Forcing Data (WFD) and three GCMs: ECHAM, CNRM and IPSL.

and arid (B) climate types where the GCM forced models show less spread in the drought characteristics than the reference model. In the snow-dominated (D) climate type a division between short duration and long multi-year drought events was found. This is caused by the fact that groundwater storage is not replenished in the winter season. Below-zero temperatures in the following summer prevent snowmelt and groundwater recharge and hence drought conditions will not lift. When summer temperatures are too low to generate enough snowmelt to replenish the groundwater, this drought will continue over the next winter. If the drought continues over winter this will automatically result in a multi-year drought and hence long drought durations (Van Loon et al., 2014). Overall, the GCM forced models show a large resemblance to the reference model throughout the climate regions, especially for the less extreme climate types. This is also illustrated through the SI (Eq. 13), when the GCM forced models are compared against the reference model (Table 2). For example, the SI for the A climate is 100 % which means that the bivariate distribution of drought duration and deficit volume for the three GCM forcing data sets is identical to the WFD forcing. The SI for the C climate is almost 100 %, and for the D climate around 90 %. For the B climate the SI is still 75 % or more, whereas for the E climate the SI is above 60 %.

The average drought duration and deficit volume for the major climates and for averaged over all climates show that the GCM forced models are in good agreement with the reference model with some mismatch in the extreme arid and polar climate types (Figs. 4 and 5). The results from Table 3 support the SI findings (Fig. 3 and Table 2) – that the GCMs are capable to produce realistic meteorological forcing for hydrological drought assessment under most climate conditions, but show difficulties in desert and polar climates. The drought duration derived from the GCM forced models for the A, C and D major climate types deviates less than 10 % from the duration obtained for the reference model (Table 2, IPSL for the A climate type is an exception). For the B and E climates the deviation is larger in particular for the latter (up to more than 50 %). The deficit volume shows a similar pattern but relative deviations are larger because of smaller magnitude (Table 2). Uncertainties in the differences are low (Table 3), increasing the confidence that bias-corrected GCM output can correctly reproduce hydrological drought characteristics for the control period.

The monthly drought deficit for the control period for all three GCM forced models shows a large similarity with the reference model derived from the WFD (Fig. 6). The GCM forced simulations show identical patterns with respect to the monthly distribution of the drought deficit. An exception is found for the polar (E) climate type, where the drought deficit volume in summer is overestimated by the GCM forced simulations.

The deviations of the GCM forcing from the reference situation that are found are most likely caused by the dis-

Table 3. Average hydrological drought characteristics for the control period (1971–2000), including relative difference for the three GCMs, relative to the WATCH Forcing Data and the standard deviation of the relative difference, derived from a two-sided *t*-test. Characteristics are provided for Equatorial (A), Arid (B), Warm temperate (C), Snow (D) and Polar climates (E).

		WFD	ECHAM	CNRM	IPSL
Duration (d)	A	54.3	57.3 (106 ± 3 %)	59.5 (110 ± 3 %)	70.7 (130 ± 10 %)
	B	79.4	57.4 (72 ± 3 %)	63.1 (79 ± 3 %)	66.5 (84 ± 4 %)
	C	50.2	49.3 (98 ± 3 %)	54.6 (109 ± 3 %)	51.4 (102 ± 3 %)
	D	57.1	56.5 (99 ± 4 %)	57.0 (100 ± 12 %)	55.5 (97 ± 6 %)
	E	105.0	48.8 (46 ± 4 %)	51.8 (49 ± 6 %)	47.2 (45 ± 4 %)
	All	66.7	59.8 (90 ± 2 %)	69.0 (103 ± 4 %)	66.6 (100 ± 2 %)
Standardized deficit volume (d)	A	5.31	4.58 (86 ± 5 %)	5.25 (99 ± 5 %)	6.61 (124 ± 6 %)
	B	8.44	4.89 (58 ± 4 %)	5.85 (69 ± 4 %)	5.47 (65 ± 4 %)
	C	4.73	4.26 (90 ± 5 %)	5.01 (106 ± 5 %)	4.13 (87 ± 5 %)
	D	5.61	4.82 (86 ± 4 %)	4.43 (79 ± 11 %)	4.14 (74 ± 5 %)
	E	10.89	4.08 (37 ± 4 %)	4.24 (39 ± 6 %)	3.64 (33 ± 4 %)
	All	6.58	5.05 (77 ± 2 %)	5.94 (90 ± 4 %)	5.24 (80 ± 2 %)

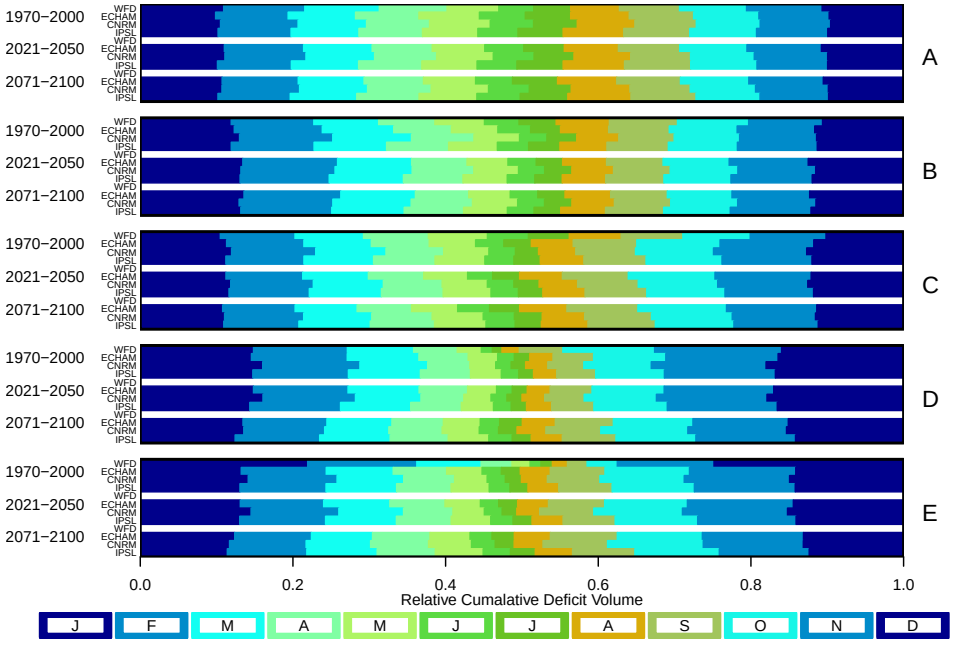

Figure 6. Monthly distribution of the annual total cumulative deficit volume over the year, obtained from simulations of the conceptual hydrological model, using meteorological forcing by the WATCH Forcing Data (WFD) and GCMs: ECHAM, CNRM and IPSL. Results are shown per analysis period and for each major climate type separately.

crepancies between the GCM forcing data and the WFD forcing. Although the bias correction removes most of these discrepancies for precipitation and temperature simulations, still differences remain. An example can be found in the co-occurrence of precipitation which is very important to lift drought conditions. When multiple drought events co-occur they are more likely to increase groundwater recharge and hence result in increased groundwater discharge. This in turn will lead to an end of a drought event, while the same precipitation volumes over a prolonged period of time would have a different effect. Since the precipitation is corrected using a fitted gamma-distribution these second-order statistics are not included in the bias correction. This could especially in dry climate have a significant impact on the drought characteristics, where a small amount of rainfall could end a drought event. In the polar climate, the interaction between precipitation amounts and temperatures is of significant importance with respect to the ending of drought events. If the forcing of the GCM were to have exactly the same higher-order statistical properties as the WFD, no differences would

Table 4. Changes in median of drought characteristics (% relative to control period, 1971–2000, including standard deviation, derived from a two-sided *t*-test) for climate types: Equatorial (A), Arid (B), Warm temperate (C), Snow (D) and Polar climates (E).

		2021–2050			2071–2100		
		ECHAM	CNRM	IPSL	ECHAM	CNRM	IPSL
Duration (d)	A	142 ± 4	138 ± 4	131 ± 12	175 ± 7	169 ± 5	181 ± 15
	B	142 ± 4	133 ± 3	144 ± 6	175 ± 6	160 ± 4	181 ± 12
	C	133 ± 4	123 ± 3	115 ± 5	150 ± 7	162 ± 6	162 ± 7
	D	107 ± 7	93 ± 15	100 ± 11	129 ± 8	121 ± 29	114 ± 12
	E	100 ± 4	108 ± 16	108 ± 8	123 ± 6	138 ± 23	131 ± 7
	All	115 ± 3	114 ± 6	121 ± 5	146 ± 3	143 ± 9	157 ± 6
PDY ($\mathrm{d\,yr^{-1}}$)	A	81 ± 5	75 ± 4	112 ± 5	74 ± 4	44 ± 4	128 ± 5
	B	95 ± 4	81 ± 3	98 ± 4	89 ± 4	56 ± 3	99 ± 4
	C	78 ± 4	65 ± 4	49 ± 3	41 ± 4	40 ± 3	22 ± 4
	D	57 ± 3	49 ± 3	47 ± 2	8 ± 3	5 ± 3	8 ± 2
	E	61 ± 4	53 ± 4	52 ± 3	22 ± 4	19 ± 4	25 ± 4
	All	70 ± 2	61 ± 1	62 ± 2	33 ± 2	26 ± 1	30 ± 2
Standardized deficit volume (d)	A	193 ± 7	194 ± 7	182 ± 25	301 ± 18	317 ± 13	327 ± 40
	B	206 ± 9	179 ± 7	218 ± 16	305 ± 15	268 ± 12	310 ± 64
	C	164 ± 10	145 ± 7	134 ± 9	217 ± 21	220 ± 20	247 ± 22
	D	131 ± 8	103 ± 18	117 ± 11	144 ± 12	152 ± 36	126 ± 25
	E	115 ± 7	128 ± 20	115 ± 8	147 ± 14	170 ± 35	167 ± 18
	All	155 ± 4	139 ± 7	146 ± 8	206 ± 7	214 ± 12	222 ± 22

occur in drought characteristics. Therefore, it is concluded that the statistical properties of the precipitation and temperature are not fully matched for the polar climates and to a lesser extent for the B-climate, which significantly impacts the drought characteristics in these climates.

4.2 Future period

All GCM forced models show a decrease in the number of hydrological droughts throughout climate types (Fig. 7, upper row, note logarithmic scale). This decreasing number of droughts is associated with an increase in the duration by 143 to 157 % for all GCM forced models in 2071–2100 (Figs. 7 and 8, second row, Table 4). The most severe droughts also show a very strong increase relative to the control period and the spread in duration between locations strongly increases (Fig. 7). The overall effect of climate change on the PDY over the two future periods shows a decreasing trend (Fig. 7, third row). The total time a location is in drought decreases by 67 to 74 % in 2071–2100 (Table 4), indicating that the locations are less in drought throughout the 30-year period (Fig. 8). The deficit volume shows an overall increase of slightly over 200 % in 2071–2100 (Table 4, Fig. 5), which indicates that although droughts are less frequent, the severity in both duration and deficit volume increases, for the remaining events. Uncertainties in the estimated relative changes are low, 2–5 % for durations and 1–5 % for the PDY (Table 4), with the exception of the deficit volume (4–64 %). This indicates that it is more difficult for the ensemble of GCMs to indicate changes in deficit volumes with high certainty.

The projected changes in the median of groundwater discharge drought characteristics (duration, deficit volume and PDY) for each major climate type are included in Table 4. The duration increases relative to the control period in all major climate regions, where the period 2071–2100 is more affected than 2021–2050 (Table 4). The strongest increase occurs for the equatorial and arid climates, where duration increases up to 181 % for IPSL (Table 4). For the snow and polar climate (D, E) the increase in duration is smaller (114–138 %) and lower than for the warmer A, B and C climates.

The PDY is projected to decrease throughout the 21st century (Fig. 8, Table 4). However, changes vary throughout climate regions. Averaged over all climates by the end of the century, median PDY will decrease to 26–33 % relative to the control period leading to an average of $\approx 22\,\mathrm{d\,yr^{-1}}$. For the equatorial climate (A) the direction of the change is not uniform. The IPSL forced model shows an increase for the equatorial climate (A) in 2071–2100 (128 %), while both ECHAM and CNRM show that the PDY will decrease throughout all climate types (74 and 44 %). For the other climate regions the direction of the change is uniform and shows a decrease in the PDY. For the snow climate, the changes are largest, the total PDY reduces to 5–8 % relative to the control period, leading to an average PDY of $\approx 5\,\mathrm{d\,yr^{-1}}$ by the end of the 21st century.

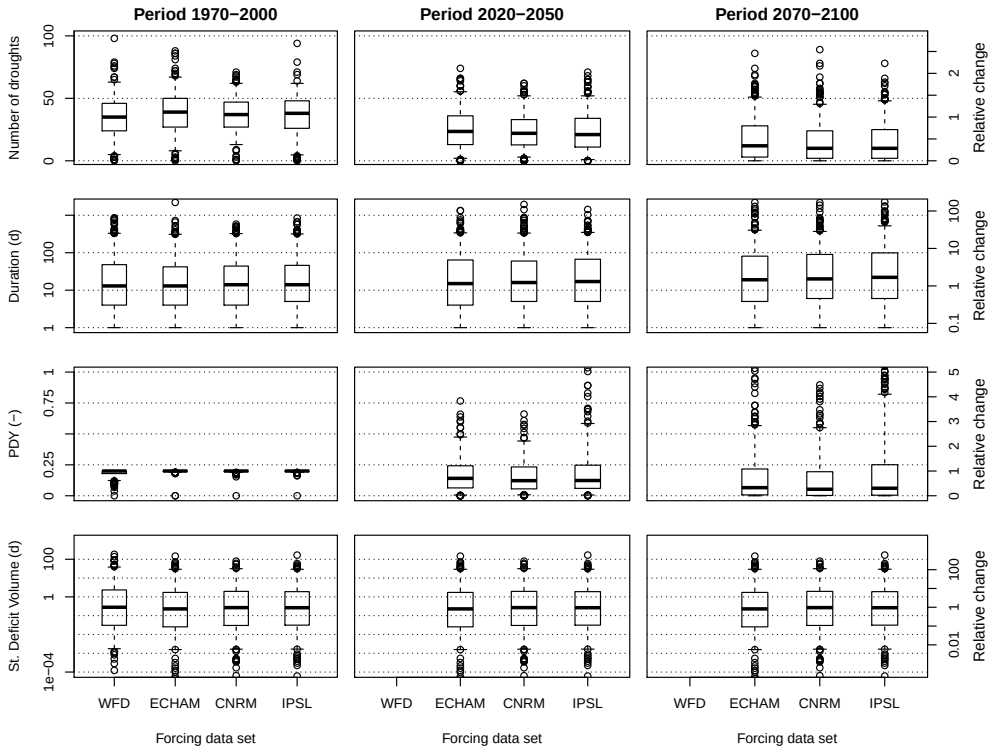

Figure 7. Distribution of three groundwater discharge drought characteristics obtained from a conceptual hydrological model using meteorological forcing from the WATCH Forcing Data (reference model) and three models with meteorological forcing from GCMs (ECHAM, CNRM and IPSL) for the control period (1971–2000). Row one indicates the number of hydrological droughts per evaluation period, row two the average drought duration (logarithmic scale), row three the percentage of the year in drought and the last row gives the average standardized deficit volume (logarithmic scale).

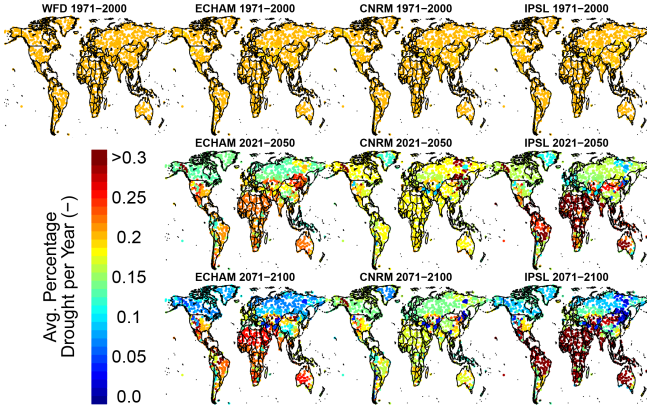

Figure 8. Spatial distribution of average percentage drought per year for different time periods, obtained from simulations of the conceptual hydrological model, using meteorological forcing by the WATCH Forcing Data (WFD) and GCMs: ECHAM, CNRM and IPSL.

A substantial increase was found for the deficit volume for all climate regions in both future periods, where the mean deficit volume clearly increases over the century (Fig. 5, Table 4). This increase is strongest for the A, B and C climates, where the ranges increase by 217–327 % leading to median deficit volumes between 9.24 and 21.6 d, i.e. 9.24 and 21.6 times the mean daily discharge. This is 2.5–6 % of the annual discharge for these regions.

Seasonal changes in the relative importance of the drought deficit are small, with the exception of the polar (E) and snow-dominated (D) climate types (Fig. 6). In these regions a shift to more spring- and summer-dominated drought are projected. This is caused by shifts in the snowmelt season due to temperature rise (as a result of climate change), resulting in a lower water availability in late spring and summer (development towards warm snow season drought, Van Loon and Van Lanen, 2012). This effect is not found in the other major climates, since the groundwater discharge seasonality in the regions is not dominated by snow accumulation and melt periods. Although locally the changes in the drought seasonality might be severe, on a global scale no changes have been found as a result of changes in climatology (e.g. shifts in precipitation patterns).

Table 5. Similarity index (SI) for the near (2021–2050) and far (2071–2100) future, compared to the control period (1971–2000) derived from a conceptual hydrological model forced with three GCMs. SI is given for all major climates: Equatorial (A), Arid (B), Warm temperate (C), Snow (D) and Polar climates (E), and averaged over all climates.

	A	B	C	D	E	All
ECHAM 2021–2050	77	71	73	84	84	81
ECHAM 2071–2100	63	60	64	70	73	69
CNRM 2021–2050	78	82	85	88	81	87
CNRM 2071–2100	64	71	68	64	68	71
IPSL 2021–2050	73	71	83	87	86	82
IPSL 2071–2100	60	58	63	73	71	68

For all future GCM forced models the 90 % probability fields were calculated and the changes relative to the control period are presented using the SI (Table 5). All models indicate that changes occur with a similar magnitude for all major climate types. For example, the SIs obtained with the ECHAM forced model show that 19 % of drought characteristics (duration and deficit volume) of events in 2021–2050 (averaged over all climates) did not occur in the control period. This percentage increases up to 31 % by the end of the century. The strongest decrease in SI (i.e. largest change) was found in the equatorial, arid and warm temperate climates (A, B, C) where SI values can be as low as 60 %. The same pattern was found for the snow climate (D) – however, changes in SI are smaller.

5 Discussion

The performance and sensitivity of the conceptual model has been evaluated in earlier studies. It was shown that the model is capable of reproducing hydrological drought characteristics in Europe and has difficulties reproducing peak flow discharges in these catchments (Tijdeman et al., 2012). Furthermore, it was found that simulated drought characteristics are most sensitive to changes in the groundwater parametrization (Van Lanen et al., 2013). The impact of meteorological forcing on the drought-generating mechanisms in the model was limited. Although the conceptual model has no real surface runoff component included in the modelling framework, this has no significant impact on the results. The hydrological droughts are mainly caused by extensive periods with low groundwater recharge, leading to reduced base flow from the catchment. This groundwater recharge is only partly influenced by the potential evaporation (as shown by Van Lanen et al., 2013). This is important because not all meteorological forcing that was used to calculate potential evaporation was bias corrected, which could impact the model simulations (Harding et al., 2014). Because the sensitivity of the model to changes in the potential evaporation and evaporation parametrization is low, the model can be used with confidence to simulate future hydrological drought characteristics.

Most global drought projections address meteorological or soil moisture drought. Dai (2013) has investigated global soil moisture drought up to 2010 and states that the PDSI changes derived from observed weather records are consistent with model predictions, which would indicate severe and extended global droughts in the 21st century resulting from either decreased precipitation and/or increased evaporation. Sheffield et al. (2012) argue that the increase in global soil moisture drought since the 1980s is overestimated because the PDSI was computed with a too simple evapotranspiration model, which has consequences of how to interpret the impact global warming on global drought changes. Orlowsky and Seneviratne (2013) use meteorological drought (SPI) and soil moisture drought (anomaly) to illustrate that there will be both wetting regions in the 21st century (e.g. East and South Asia, Sahel, Central North America, Central Europe) and drying regions (e.g. Australia, South Africa, Central America, Amazon, Mediterranean). Seneviratne et al. (2012) conclude that there is medium confidence that in some regions across the world duration and intensity of meteorological or soil moisture drought will increase and elsewhere the confidence level is low because of definitional differences or model disagreement. Land surface processes and properties, e.g. groundwater flow and storage, and stream–aquifer interaction (Van Lanen et al., 2004; Van Loon et al., 2012), make meteorological or soil moisture drought projections not straightforwardly applicable to hydrological droughts.

Hydrological drought projections, which are of paramount importance for assessments of future water resources, are still limited. Hydrological drought projections are often associated with change in annual runoff or river flow (e.g. Hagemann et al., 2013; Schewe et al., 2014). Off-line approaches on a global scale use large-scale hydrological models in combination with forcing from either GCMs or RCMs. Intermediate approaches are needed to downscale and bias correct the climate model forcing (Haddeland et al., 2011), which is a challenging process (e.g. Sperna Weiland et al., 2010; Hagemann et al., 2011), in particular for the future climate (Chen et al., 2011). Some attempts have been made to derive hydrological drought characteristics at the global or continental scale under future climate. Forzieri et al. (2014) project an increase in deficit volume of river flow for vast areas of Europe, except the Scandinavian countries and North Russia. Hirabayashi et al. (2008) and Feyen and Dankers (2009) project a substantial increase in the number of drought days (PDY) or flow deficit volume for the period 2071–2100 in some regions, whereas in contrast, wide areas will benefit from a decrease in drought days. An increase in number of drought days in general is not in line with the modelling experiment in this study, whereas an increase in deficit volume is supported (Table 4). In a preliminary study Corzo Perez et al. (2011b) analysed future drought for two time domains

(2021–2050 and 2071–2100), two emission scenarios (A2 and B1), three downscaled and bias-corrected GCMs, and five large-scale hydrological models. The number and spatial distribution of drought events did not clearly show a consistent change. As part of the ISI-MIP project, Prudhomme et al. (2014) used an ensemble of GCM–GHM combinations and found that drought occurrence will increase globally with the exception of the snow-dominated regions. Strong increases in drought occurrence are found for the Mediterranean region, which is confirmed by this study. Using a multi-GCM approach with an adapted drought threshold approach using a gradually changing hydrological regime, Wanders et al. (2015) found increased water availability in the colder snow-dominated climate types, which is in line with the findings of this study. However, more research into this topic is certainly needed and additional data sets are required to fully understand the impact of the uncertainties and their impact on future hydrological drought. Moreover, the impact of humans on future hydrological drought has only been recently studied and is believed to have a significant impact on future water resources and related hydrological drought (e.g. Hagemann et al., 2013; Haddeland et al., 2014; Schewe et al., 2014; Wanders and Wada, 2014).

In the control period 1971–2000, differences occur between hydrological drought characteristics (Fig. 3) derived from groundwater discharge time series simulated with meteorological forcing from downscaled and bias-corrected outcome from three general circulation models (GCM forced models). For example, the duration and deficit volume averaged over all climates varies from 60 to 69 d and 5.05 to 5.94 d, respectively, for the three GCM forced models (Table 3). The main reason for this is GCM model uncertainty, caused by the differences in model structures (Chen et al., 2011; Haerter et al., 2011). Agreement in the directionality of the changes in future hydrological drought characteristics among GCM forced models are more similar than agreement in the control period between GCM forced models and characteristics that were obtained using re-analysis data as meteorological forcing (reference model). Exceptions are the B and E climates (Tables 2 and 3). For the A, C and D climates differences in drought duration of GCM forced models against the reference model vary from 0to 30 %, whereas for the deficit volume the range is 1 to 26 % (Figs. 4 and 5). Differences in drought characteristics between GCM forced models and the reference model are mostly negative, implying that the drought duration and standard deficit volume are smaller when GCM forcing was used instead of re-analysis data. Differences in drought characteristics against the reference model are not always mono-directional for a particular climate (e.g. drought duration for the C climate). The above-mentioned differences are a measure for climate model uncertainty. Most large-scale studies, which explore hydrological impact of climate change, compare simulated and observed annual river flow to assess model fitness as a basis for projections (e.g. Arnell, 2003; Milly et al., 2005; Hagemann et al., 2013; Schewe et al., 2014). Other studies also focus on low water availability and include minimum flow or flow deficits to investigate future drought (e.g Feyen and Dankers, 2009; Forzieri et al., 2014). Few large-scale studies test hydrological model performance by comparing GCM forcing against observed forcing. Sperna Weiland et al. (2010) are such an exception. They conclude that bias-corrected GCM forcing should be used with caution for global hydrological impact studies in which persistence is relevant, like for drought. Another example is Corzo Perez et al. (2011b), who confirm that for a control period no clear patterns can be found in differences between hydrological drought characteristics derived from GCM-forced hydrological models and the same models forced with re-analysis data.

Global annual precipitation totals is projected to increase throughout the 21st century, although locally annual precipitation might decrease (Solomon et al., 2007). Precipitation increase is most prominent in the equatorial and polar climates, resulting in an increase in discharge (Solomon et al., 2007), which was confirmed by the data from GCMs that we used for this study. Therefore, in the 21st century the historic Q_{80} (1971–2000) was exceeded for more than 80 % of the time in our study, hence the PDY decreased both in the near and far future (Table 4).

It was noticed that for the equatorial climate the impact of climate change is not unambiguous. Two GCM forced models (ECHAM, CNRM) indicate a decrease in total drought occurrence (PDY) relative to the control period (19–25 % for 2012–2050 and 36–56 % for 2071–2100), while one GCM forced model (IPSL) indicates a small increase (12 % for 2012–2050 and 28 % for 2071–2100) in total drought occurrence (A climate, Table 4). The main reason for the model disagreement is an increase in precipitation projected by ECHAM and CNRM and a decrease by IPSL in most of the selected locations for the A climate leading to higher and lower discharge, respectively.

The three GCMs project increasing annual temperatures leading to a decreased length of the snow accumulation period in cold climates (D and E climates), which have great impact on river flow (e.g. Wilson et al., 2010), and consequently on drought occurrence (PDY, D climates, Table 4). For instance, duration of rain-to-snow-season droughts as identified by Van Loon and Van Lanen (2012) will decrease due to later precipitation as rain in autumn or earlier rain in spring, leading to quicker snowmelt peak. It was found that the combined effect of increased precipitation and shorter snow accumulation periods causes a strong decrease in total drought duration (i.e. PDY). Feyen and Dankers (2009) report on a decrease in drought severity (i.e. 7-day minimum flow and deficit volume during the frost period) in the cold European climates. Classical rainfall droughts, however, will become more severe due to lower summer flows in some regions, e.g. southern and eastern Norway (Feyen and Dankers, 2009; Wilson et al., 2010; Wong et al., 2011; Stahl et al., 2011), which is supported by this study, where the remain-

ing droughts in the far future last 14–29 % longer and are 26–52 % more severe.

A large portion of the globe is covered by snow-dominated and polar climates (D and E, Fig. 2). While the impact of climate change on hydrological drought may be most severe for the snow-dominated regions (D and E climates), the societal impact is expected to be relatively low. In these regions the population density is low and the projected changes have a positive impact on the water availability. Projected changes are far more likely to have a significant impact on the tropical and desert climates (A and B climate). In these regions vulnerability to drought is higher while the drought resilience is lower compared to other regions in the world. Therefore, the forecasted increase in severity and duration of drought should be seen as events which could severely impact the region. These changes could lead to forced immigration, putting pressure on adjacent regions usually also scarce in water already. Uncertainty in projections for these regions should challenge policy makers and stakeholders to take appropriate decisions for drought adaptation measures.

6 Conclusions

With a synthetic hydrological modelling approach, the impact of climate change on drought occurrence and severity was studied. Drought characteristics of drought duration, standardized deficit volume and percentage of drought occurrence per year were calculated for the time period 1960–2100. Three different GCMs (ECHAM, CNRM, IPSL) were used as meteorological forcing to simulate possible effects of climate change on droughts (GCM forced models). The A2 emission scenario was used to explore the most severe outcome for the three GCM forced models. Obtained drought characteristics were compared against the drought characteristics obtained from simulations of the hydrological model forced with meteorological data from the WATCH Forcing Data set, which was used as a reference data set in this study (reference model). Comparison was performed for the control period 1971–2000 and the deviations of each GCM forced model from the reference model were calculated. On a global scale drought duration found for the reference model and the GCM forced models were of the same order of magnitude, while the standardized deficit volume was underestimated compared against the reference model. It was concluded that the GCM forced models produce realistic meteorological forcing for future hydrological drought assessment, but have difficulties in capturing the more extreme arid and polar climates. This issue is most likely caused by the fact that second-order statistics like the sequence of rainfall events, and the co-occurrence and magnitude of specific events is different compared to the WATCH Forcing Data. These second-order statistics could have significant impact on the duration and severity of hydrological drought events and are difficult to correct in a bias-correction approach.

The effects of climate change were studied for two periods, namely 2021–2050 and 2071–2100, and compared relative to the control period. From the analysis it is concluded that average drought duration and standardized deficit volume will increase as a result of climate change. However, the total drought duration and number of droughts will decrease since on a global scale the total water availability will increase due to increased precipitation totals.

On a global scale the average duration of drought events will increase by a factor of 1.5 in the far future (2071–2100), where this increase is most severe in the equatorial and arid climate types. Overall the total drought duration (PDY) decreases to 26–33 % relative to the control period, where the decrease is most striking in the snow climates. Increasing temperatures cause a decrease in winter droughts and snow accumulation, combined with increase precipitation leading to a very strong decrease in total drought duration (5–8 % relative to the control period). Global average drought standardized deficit volume increases by slightly more than 2 times for the period 2071–2100, which suggests that drought severity will increase as a result of changes in the climate.

Projections of global hydrological drought, which are essential for future water resource management, are still very limited. This study advances the knowledge on future hydrological drought. Averaged over all climates, the bias-corrected GCM forced hydrological models produce similar changes in discharge drought. Some spread is found among the models, but the directionality is similar. In general, the synthetic hydrological modelling approach shows that hydrological drought occurrence (i.e. total days in drought per year) is projected to decrease over the 21st century, particularly in the temperate and cold climate regions. In contrast, average drought duration and deficit volume of the remaining droughts are expected to substantially increase. The most critical impacts are projected for the already water-scarce arid climates (B climates), where drought occurrence will not decrease that much and average duration and deficit volume of remaining drought events will increase more than in other climates. However, in this climate, model uncertainty is largest.

Acknowledgements. The authors would like to thank Graham Weedon (UK MetOffice) for supplying the WATCH Forcing Data. We appreciate very much the work done by Cui Chen, Jan Haerter and Stefan Hagemann (Terrestrial Hydrology Group, Max Planck Institute for Meteorology, Hamburg, Germany), Jens Heinke (Potsdam Institute for Climate Impact Research, Potsdam, Germany) and Claudio Piani (Abdus Salam International Centre for Theoretical Physics, Trieste, Italy) to downscale and bias correct the climate output from the three GCMs (daily data, 1960–2100) used in this study. This research has been financially supported by the EU-FP6 Project WATCH (contract 036946), the EU-FP7 Project DROUGHT-R&SPI (contract 282769) and NWO (NWO GO-AO/30). This research supports the work of the UNESCO-IHP VIII FRIEND-Water programme.

Edited by: U. Ulbrich
Reviewed by: six anonymous referees

References

Alderlieste, M. A. A., Van Lanen, H. A. J., and Wanders, N.: Future low flows and hydrological drought: how certain are these for Europe, in: Hydrology in a Changing World: Environmental and Human Dimensions, edited by: Daniell, T., Van Lanen, H., Demuth, S., Laaha, G., Servat, E., Mahe, G., Boyer, J.-F., Paturel, J.-E., Dezetter, A., and Ruelland, D., no. 363 in IAHS Publications, 60–65, 2014.

Allen, R., Pereira, L., Raes, D., and Smith, M.: FAO Irrigation and Drainage Paper No. 56 – Crop Evapotranspiration, Food and Agriculture Organization, 2006.

Andreadis, K. M., Clark, E. A., Wood, A. W., Hamlet, A. F., and Lettenmaier, D. P.: Twentieth-Century Drought in the Conterminous United States, J. Hydrometeorol., 6, 985–1001, doi:10.1175/JHM450.1, 2005.

Arnell, N. W.: Effects of IPCC SRES* emissions scenarios on river runoff: a global perspective, Hydrol. Earth Syst. Sci., 7, 619–641, doi:10.5194/hess-7-619-2003, 2003.

Chen, F., Crow, W. T., Starks, P. J., and Moriasi, D. N.: Improving hydrologic predictions of a catchment model via assimilation of surface soil moisture, Adv. Water Resour., 34, 526–536, doi:10.1016/j.advwatres.2011.01.011, 2011.

Clyde, G.: Snow Melting Characteristics, Utah Agricultural Experiment Station bulletin, 231, 1–23, 1931.

Collins, E. H.: Relationship of degree-days above freezing to runoff., Transactions of the American Geophysical Union, Reports and Papers, Hydrology, 15, 624–629, 1934.

Corzo Perez, G. A., van Huijgevoort, M. H. J., Voß, F., and van Lanen, H. A. J.: On the spatio-temporal analysis of hydrological droughts from global hydrological models, Hydrol. Earth Syst. Sci., 15, 2963–2978, doi:10.5194/hess-15-2963-2011, 2011a.

Corzo Perez, G. A., Van Lanen, H. A. J., Bertrand, N., Chen, C., Clark, D., Folwell, S., Gosling, S. N., Hanasaki, N., Heinke, J., and Voß, F.: Drought at the global scale in the 21st Century, Tech. Rep. 43, EU WATCH (Water and global Change) project, 2011b.

Dai, A.: Drought under global warming: a review, Wiley Interdisciplinary Reviews: Climate Change, 2, 45–65, doi:10.1002/wcc.81, 2011.

Dai, A.: Increasing drought under global warming in observations and models, Nat. Clim. Change, 3, 52–58, doi:10.1038/nclimate1633, 2013.

Dai, A., Trenberth, K., and Qian, T.: A global dataset of Palmer Drought Severity Index for 1870–2002: Relationship with soil moisture and effects of surface warming, J. Hydrometeorol., 5, 1117–1130, 2004.

EEA: Mapping the impact of natural hazards and technological accidents in Europe. An overview of the last decade, Tech. Rep. 13/2010, EEA, Copenhagen, 2010.

Feyen, L. and Dankers, R.: Impact of global warming on streamflow drought in Europe, J. Geophys. Res.-Space Phys., 114, D17116, doi:10.1029/2008JD011438, 2009.

Fichefet, T. and Maqueda, M. A. M.: Sensitivity of a global sea ice model to the treatment of ice thermodynamics and dynamics, J. Geophys. Res.-Space Phys., 102, 12609–12646, doi:10.1029/97JC00480, 1997.

Fleig, A. K., Tallaksen, L. M., Hisdal, H., and Demuth, S.: A global evaluation of streamflow drought characteristics, Hydrol. Earth Syst. Sci., 10, 535–552, doi:10.5194/hess-10-535-2006, 2006.

Forzieri, G., Feyen, L., Rojas, R., Flörke, M., Wimmer, F., and Bianchi, A.: Ensemble projections of future streamflow droughts in Europe, Hydrol. Earth Syst. Sci., 18, 85–108, doi:10.5194/hess-18-85-2014, 2014.

Geiger, R.: Klassifikation der Klimate nach W. Köppen, in: Landolt-Börnstein Zahlenwerte und Funktionen aus Physik, Chemie, Astronomie, Geophysik und Technik, Vol. 3 of alte Serie, Chap. Klassifikation der Klimate nach W. Köppen, 603–607, Springer, Berlin, 1954.

Geiger, R.: Überarbeitete Neuausgabe von Geiger, R.: Köppen-Geiger/ Klima der Erde, Wandkarte 1 : 16 Mill., klett-Perthes, Gotha, 1961.

Goosse, H. and Fichefet, T.: Importance of ice-ocean interactions for the global ocean circulation: A model study, J. Geophys. Res.-Space Phys., 104, 23337–23355, doi:10.1029/1999JC900215, 1999.

Gudmundsson, L., Tallaksen, L. M., Stahl, K., Clark, D. B., Dumont, E., Hagemann, S., Bertrand, N., Gerten, D., Heinke, J., Hanasaki, N., Voss, F., and Koirala, S.: Comparing Large-Scale Hydrological Model Simulations to Observed Runoff Percentiles in Europe, J. Hydrometeorol., 13, 604–620, doi:10.1175/JHM-D-11-083.1, 2012.

Haddeland, I., Clark, D. B., Franssen, W., Ludwig, F., Voß, F., Arnell, N. W., Bertrand, N., Best, M., Folwell, S., Gerten, D., Gomes, S., Gosling, S. N., Hagemann, S., Hanasaki, N., Harding, R., Heinke, J., Kabat, P., Koirala, S., Oki, T., Polcher, J., Stacke, T., Viterbo, P., Weedon, G. P., and Yeh, P.: Multimodel Estimate of the Global Terrestrial Water Balance: Setup and First Results, J. Hydrometeorol., 12, 869–884, doi:10.1175/2011JHM1324.1, 2011.

Haddeland, I., Heinke, J., Biemans, H., Eisner, S., Flörke, M., Hanasaki, N., Konzmann, M., Ludwig, F., Masaki, Y., Schewe, J., Stacke, T., Tessler, Z. D., Wada, Y., and Wisser, D.: Global water resources affected by human interventions and climate change, P. Natl. Acad. Sci., 111, 3251–3256, doi:10.1073/pnas.1222475110, 2014.

Haerter, J. O., Hagemann, S., Moseley, C., and Piani, C.: Climate model bias correction and the role of timescales, Hydrol. Earth Syst. Sci., 15, 1065–1079, doi:10.5194/hess-15-1065-2011, 2011.

Hagemann, S., Chen, C., Haerter, J. O., Heinke, J., Gerten, D., and Piani, C.: Impact of a Statistical Bias Correction on the Projected Hydrological Changes Obtained from Three GCMs and Two Hydrology Models, J. Hydrometeorol., 12, 556–578, doi:10.1175/2011JHM1336.1, 2011.

Hagemann, S., Chen, C., Clark, D. B., Folwell, S., Gosling, S. N., Haddeland, I., Hanasaki, N., Heinke, J., Ludwig, F., Voss, F., and Wiltshire, A. J.: Climate change impact on available water resources obtained using multiple global climate and hydrology models, Earth Syst. Dynam., 4, 129–144, doi:10.5194/esd-4-129-2013, 2013.

Hannah, D. M., Demuth, S., van Lanen, H. A. J., Looser, U., Prudhomme, C., Rees, G., Stahl, K., and Tallaksen, L. M.: Large-scale

river flow archives: importance, current status and future needs, Hydrol. Process., 25, 1191–1200, doi:10.1002/hyp.7794, 2011.

Harding, R., Best, M., Blyth, E., Hagemann, S., Kabat, P., Tallaksen, L. M., Warnaars, T., Wiberg, D., Weedon, G. P., Lanen, H. v., Ludwig, F., and Haddeland, I.: WATCH: Current Knowledge of the Terrestrial Global Water Cycle, J. Hydrometeorol., 12, 1149–1156, doi:10.1175/JHM-D-11-024.1, 2011.

Harding, R. J., Weedon, G. P., van Lanen, H. A., and Clark, D. B.: The future for global water assessment, Special Issue: Climatic change impact on water: Overcoming data and science gaps, J. Hydrol., 518, Part B, 186–193, doi:10.1016/j.jhydrol.2014.05.014, 2014.

Hirabayashi, Y., Kanae, S., Emori, S., Oki, T., and Kimoto, M.: Global projections of changing risks of floods and droughts in a changing climate, Hydrol. Sci. J., 53, 754–772, 2008.

Hisdal, H., Tallaksen, L. M., Clausen, B., Peters, E., and Gustard, A.: Hydrological Drought Characteristics, in: Hydrological Drought: Processes and estimation methods for streamflow and groundwater, edited by: Tallaksen, L. M. and Van Lanen, H. A. J., no. 48 in Development in Water Science, 139–198, Elsevier, Amsterdam, the Netherlands, 2004.

Hourdin, F., Musat, I., Bony, S., Braconnot, P., Codron, F., Dufresne, J.-L., Fairhead, L., Filiberti, M.-A., Friedlingstein, P., Grandpeix, J.-Y., Krinner, G., LeVan, P., Li, Z.-X., and Lott, F.: The LMDZ4 general circulation model: climate performance and sensitivity to parametrized physics with emphasis on tropical convection, Clim. Dynam., 27, 787–813, doi:10.1007/s00382-006-0158-0, 2006.

Jungclaus, J. H., Keenlyside, N., Botzet, M., Haak, H., Luo, J.-J., Latif, M., Marotzke, J., Mikolajewicz, U., and Roeckner, E.: Ocean Circulation and Tropical Variability in the Coupled Model ECHAM5/MPI-OM, J. Climate, 19, 3952–3972, doi:10.1175/JCLI3827.1, 2006.

Köppen, W.: Versuch einer Klassifikation der Klimate, vorzugsweise nach ihren Beziehungen zur Pflanzenwelt, Geografische Z., 6, 593–611, 657–679, 1900.

Kraijenhof van de Leur, D.: Some effects of the unsaturated zone on nonsteady free-surface groundwater flow as studied in a sealed granular model, J. Geophys. Res.-Space Phys., 67, 4347–4362, 1962.

Madec, G., Delecluse, P., Imbard, M., and Lévy, C.: OPA version 8.1 Ocean General Circulation Model reference manual, University Paris VI, Paris, notes du pole de model, 11th Edn., 1998.

McKee, T., Doesken, N., and Kleist, J.: The relationship of drought frequency and duration to time scales, in: Eighth Conference on Applied Climatology, 17–22 January, Anaheim, California, 1993.

McMahon, T. A., Peel, M. C., Lowe, L., Srikanthan, R., and McVicar, T. R.: Estimating actual, potential, reference crop and pan evaporation using standard meteorological data: a pragmatic synthesis, Hydrol. Earth Syst. Sci., 17, 1331–1363, doi:10.5194/hess-17-1331-2013, 2013.

Milly, P. C. D., Dunne, K. A., and Vecchia, A. V.: Global pattern of trends in streamflow and water availability in a changing climate, Nature, 438, 347–350, doi:10.1038/nature04312, 2005.

Mishra, A. K. and Singh, V. P.: A review of drought concepts, J. Hydrol., 391, 202–216, doi:10.1016/j.jhydrol.2010.07.012, 2010.

Mitchell, T. and Jones, P.: An improved method of constructing a database of monthly climate observations and associated high-resolution grids, Int. J. Climatol., 25, 693–712, 2005.

Nakićenović, N. and Swart, R.: Special Report on Emissions Scenarios: A special report of Working Group III of the Intergovernmental Panel on Climate Change, Cambridge University Press, 2000.

Nash, J. and Sutcliffe, J.: River flow forecasting through conceptual models part I: A discussion of principles, J. Hydrol., 10, 282–290, doi:10.1016/0022-1694(70)90255-6, 1970.

National Oceanic and Atmospheric Administration, available at: www.ncdc.noaa.gov/sotc/drought/2012 (last access: 14 November 2014), 2012.

Orlowsky, B. and Seneviratne, S. I.: Elusive drought: uncertainty in observed trends and short- and long-term CMIP5 projections, Hydrol. Earth Syst. Sci., 17, 1765–1781, doi:10.5194/hess-17-1765-2013, 2013.

Palmer, W.: Meteorological drought, U.S. Weather Bureau Research Paper, No. 45, 58 pp., 1965.

Parry, S., Prudhomme, C., Hannaford, J., and Lloyd-Hughes, B.: Examining the spatio-temporal evolution and characteristics of large-scale European droughts, in: Role of Hydrology in Managing Consequences of a Changing Global Environment. Proceedings of the BHS Third International Symposium, edited by: Kirby, C., 135–142, British Hydrological Society, 2010.

Peters, E., Torfs, P. J. J. F., van Lanen, H. A. J., and Bier, G.: Propagation of drought through groundwater – a new approach using linear reservoir theory, Hydrol. Process., 17, 3023–3040, 2003.

Piani, C., Haerter, J., and Coppola, E.: Statistical bias correction for daily precipitation in regional climate models over Europe, Theor. Appl. Climatol., 99, 187–192, doi:10.1007/s00704-009-0134-9, 2010a.

Piani, C., Weedon, G., Best, M., Gomes, S., Viterbo, P., Hagemann, S., and Haerter, J.: Statistical bias correction of global simulated daily precipitation and temperature for the application of hydrological models, J. Hydrol., 395, 199–215, doi:10.1016/j.jhydrol.2010.10.024, 2010b.

Prudhomme, C., Parry, S., Hannaford, J., Clark, D. B., Hagemann, S., and Voss, F.: How Well Do Large-Scale Models Reproduce Regional Hydrological Extremes in Europe?, J. Hydrometeorol., 12, 1181–1204, doi:10.1175/2011JHM1387.1, 2011.

Prudhomme, C., Giuntoli, I., Robinson, E. L., Clark, D. B., Arnell, N. W., Dankers, R., Fekete, B. M., Franssen, W., Gerten, D., Gosling, S. N., Hagemann, S., Hannah, D. M., Kim, H., Masaki, Y., Satoh, Y., Stacke, T., Wada, Y., and Wisser, D.: Hydrological droughts in the 21st century, hotspots and uncertainties from a global multimodel ensemble experiment, P. Natl. Acad. Sci., 111, 3262–3267, doi:10.1073/pnas.1222473110, 2014.

Ritzema, H.: Subsurface Flow to Drains, in: Drainage Principles and Applications, edited by: Ritzema, H., 263–303, International Institute for Land Reclamation and Improvement, 2nd Edn., 1994.

Roeckner, E., Bäuml, G., Bonaventura, L., Brokopf, R., Esch, M., Giorgetta, M., Hagemann, S., Kirchner, I., Kornblueh, L., Manzini, E., Rhodin, A., Schlese, U., Schulzweida, U., and Tompkins, A.: The atmospheric general circulation model ECHAM5 Part I, Tech. Rep. 349, Max-Planck-Institut für Meteorologie, 2003.

Romm, J.: Desertification: The next dust bowl, Nature, 478, 450–451, doi:10.1038/478450a, 2011.

Royer, J.-F., Cariolle, D., Chauvin, F., Déqué, M., Douville, H., Hu, R.-M., Planton, S., Rascol, A., Ricard, J.-L., Melia, D. S. Y., Sevault, F., Simon, P., Somot, S., Tyteca, S., Terray, L., and Valcke, S.: Simulation des changements climatiques au cours du XXIe siècle incluant l'ozone stratosphérique, Compt. Rendus Geosci., 334, 147–154, doi:10.1016/S1631-0713(02)01728-5, 2002.

Salas-Mélia, D.: A global coupled sea ice-ocean model, Ocean Modell., 4, 137–172, doi:10.1016/S1463-5003(01)00015-4, 2002.

Schewe, J., Heinke, J., Gerten, D., Haddeland, I., Arnell, N. W., Clark, D. B., Dankers, R., Eisner, S., Fekete, B. M., Colón-González, F. J., Gosling, S. N., Kim, H., Liu, X., Masaki, Y., Portmann, F. T., Satoh, Y., Stacke, T., Tang, Q., Wada, Y., Wisser, D., Albrecht, T., Frieler, K., Piontek, F., Warszawski, L., and Kabat, P.: Multimodel assessment of water scarcity under climate change, P. Natl. Acad. Sci., 111, 3245–3250, doi:10.1073/pnas.1222460110, 2014.

Schneider, U., Fuchs, T., Meyer-Christoffer, A., and Rudolf, B.: Global precipitation analysis products of the GPCC, Global Precipitation Climatology Centre (GPCC), available at: gpcc.dwd.de (last access: 15 February 2012), 2008.

Seibert, J.: HBV light version 2 User's Manual, Stockholm University, Department of Physical Geography and Quaternary Geology, 2002.

Seneviratne, S. I., Nicholls, N., Easterling, D., Goodess, C. M., Kanae, S., Kossin, J., Luo, Y., Marengo, J., McInnes, K., Rahimi, M., Reichstein, M., Sorteberg, A., Vera, C., and Zhang, X.: Changes in climate extremes and their impacts on the natural physical environment, chap. A Special Report of Working Groups I and II of the Intergovernmental Panel on Climate Change (IPCC), 109–230, Cambridge University Press, Cambridge, UK, and New York, NY, USA, 2012.

Sheffield, J. and Wood, E. F.: Drought: Past Problems and Future Scenarios, Earthscan, London, 2011.

Sheffield, J. and Wood, F.: Characteristics of global and regional drought, 1950–2000: Analysis of soil moisture data from off-line simulation of the terrestrial hydrologic cycle, J. Geophys. Res.-Space Phys., 112, D17115, doi:10.1029/2006JD008288, 2007.

Sheffield, J., Andreadis, K., Wood, E., and Lettenmaier, D.: Global and continental drought in the second half of the twentieth century: Severity-Area-Duration analysis and temperol variability of large-scale events, J. Climate, 22, 1962–1981, 2009.

Sheffield, J., Wood, E. F., and Roderick, M. L.: Little change in global drought over the past 60 years, Nature, 491, 435–438, doi:10.1038/nature11575, 2012.

Solomon, S., Qin, D., Manning, M., Chen, Z., Marquis, M., Averyt, K., Tignor, M., and Miller, H.: Contribution of Working Group I to the Fourth Assessment Report of the Intergovernmental Panel on Climate Change, 2007, Tech. Rep., IPCC, Cambridge, United Kingdom and New York, NY, USA, 2007.

Sperna Weiland, F. C., van Beek, L. P. H., Kwadijk, J. C. J., and Bierkens, M. F. P.: The ability of a GCM-forced hydrological model to reproduce global discharge variability, Hydrol. Earth Syst. Sci., 14, 1595–1621, doi:10.5194/hess-14-1595-2010, 2010.

Stahl, K., Tallaksen, L. M., Gudmundsson, L., and Christensen, J. H.: Streamflow Data from Small Basins: A Challenging Test to High-Resolution Regional Climate Modeling, J. Hydrometeorol., 12, 900–912, doi:10.1175/2011JHM1356.1, 2011.

Stahl, K., Tallaksen, L. M., Hannaford, J., and van Lanen, H. A. J.: Filling the white space on maps of European runoff trends: estimates from a multi-model ensemble, Hydrol. Earth Syst. Sci., 16, 2035–2047, doi:10.5194/hess-16-2035-2012, 2012.

Tallaksen, L. M. and Van Lanen, H. A. J.: Hydrological Drought: Processes and estimation methods for streamflow and groundwater, no. 48 in Development in water science, Elsevier, 2004.

Tallaksen, L. M., Madsen, H., and Clausen, B.: On the definition and modelling of streamflow drought duration and deficit volume, Hydrol. Sci., 42, 15–33, 1997.

Tallaksen, L. M., Hisdal, H., and Van Lanen, H. A. J.: Space-time modelling of catchment scale drought characteristics, J. Hydrol., 375, 363–372, 2009.

Tijdeman, E., Van Loon, A. F., Wanders, N., and Van Lanen, H. A. J.: The effect of climate on droughts and their propagation in different parts of the hydrological cycle, Tech. Rep. 2, EU-Drought-R-SPI, 2012.

United Nations: Humanitarian Requirements for the Horn of Africa Drought 2011, Tech. Rep., Office for the Coordination of Humanitarian Affairs (OCHA), New York and Geneva, 2011.

Uppala, S. M., Kallberg, P. W., Simmons, A. J., Andrae, U., Bechtold, V. D. C., Fiorino, M., Gibson, J. K., Haseler, J., Hernandez, A., Kelly, G. A., Li, X., Onogi, K., Saarinen, S., Sokka, N., Allan, R. P., Andersson, E., Arpe, K., Balmaseda, M. A., Beljaars, A. C. M., Berg, L. V. D., Bidlot, J., Bormann, N., Caires, S., Chevallier, F., Dethof, A., Dragosavac, M., Fisher, M., Fuentes, M., Hagemann, S., Hólm, E., Hoskins, B. J., Isaksen, L., Janssen, P. A. E. M., Jenne, R., McNally, A. P., Mahfouf, J. F., Morcrette, J. J., Rayner, N. A., Saunders, R. W., Simon, P., Sterl, A., Trenberth, K. E., Untch, A., Vasiljevic, D., Viterbo, P., and Woollen, J.: The ERA-40 re-analysis, Q. J. Roy. Meteorol. Soc., 131, 2961–3012, 2005.

Van Huijgevoort, M. H. J., Hazenberg, P., Van Lanen, H. A. J., and Uijlenhoet, R.: A generic method for hydrological drought identification across different climate regions, Hydrol. Earth Syst. Sci., 16, 2437–2451, doi:10.5194/hess-16-2437-2012, 2012.

Van Huijgevoort, M. H. J., Hazenberg, P., van Lanen, H. A. J., Teuling, A. J., Clark, D. B., Folwell, S., Gosling, S. N., Hanasaki, N., Heinke, J., Koirala, S., Stacke, T., Voss, F., Sheffield, J., and Uijlenhoet, R.: Global Multimodel Analysis of Drought in Runoff for the Second Half of the Twentieth Century, J. Hydrometeorol., 14, 1535–1552, doi:10.1175/JHM-D-12-0186.1, 2013.

Van Huijgevoort, M. H. J., Van Lanen, H. A. J., Teuling, A. J., and Uijlenhoet, R.: Identification of changes in hydrological drought characteristics from a multi-GCM driven ensemble constrained by observed discharge, J. Hydrol., 512, 421–434, doi:10.1016/j.jhydrol.2014.02.060, 2014.

Van Lanen, H. A. J., M., F., Kupczyk, E., Kasprzyk, A., and Pokojski, W.: Flow generating processes, in: Hydrological Drought: Processes and estimation methods for streamflow and groundwater, edited by: Tallaksen, L. M. and van Lanen, H. A. J., no. 48 in Development in Water Science, 53–98, Elsevier, 2004.

Van Lanen, H. A. J., Wanders, N., Tallaksen, L. M., and Van Loon, A. F.: Hydrological drought across the world: impact of climate and physical catchment structure, Hydrol. Earth Syst. Sci., 17, 1715–1732, doi:10.5194/hess-17-1715-2013, 2013.

Van Loon, A. F. and Van Lanen, H. A. J.: A process-based typology of hydrological drought, Hydrol. Earth Syst. Sci., 16, 1915–1946, doi:10.5194/hess-16-1915-2012, 2012.

Van Loon, A. F., Van Huijgevoort, M. H. J., and Van Lanen, H. A. J.: Evaluation of drought propagation in an ensemble mean of large-scale hydrological models, Hydrol. Earth Syst. Sci., 16, 4057–4078, doi:10.5194/hess-16-4057-2012, 2012.

Van Loon, A. F., Tijdeman, E., Wanders, N., Van Lanen, H. A. J., Teuling, A. J., and Uijlenhoet, R.: How Climate Seasonality Modifies Drought Duration and Deficit, J. Geophys. Res.-Atmos., 119, 4640–4656, doi:10.1002/2013JD020383, 2014.

Van Vliet, M. T. H., Yearsley, J. R., Ludwig, F., Vogele, S., Lettenmaier, D. P., and Kabat, P.: Vulnerability of US and European electricity supply to climate change, Nat. Clim. Change, 2, 676–681, doi:10.1038/nclimate1546, 2012.

Wand, M. P. and Jones, M. C.: Kernel Smoothing, Chapman and Hall, London, 1995.

Wanders, N. and Wada, Y.: Human and climate impacts on the 21st century hydrological drought, J. Hydrol., doi:10.1016/j.jhydrol.2014.10.047, in press, 2014.

Wanders, N., Wada, Y., and Van Lanen, H. A. J.: Global hydrological droughts in the 21st century under a changing hydrological regime, Earth Syst. Dynam., 6, 1–15, doi:10.5194/esd-6-1-2015, 2015.

Weedon, G., Gomes, S., Viterbo, P., Österle, H., Adam, J., Bellouin, N., Boucher, O., and Best, M.: The WATCH Forcing Data 1958-2001: A Meteorological forcing dataset for land surface- and hydrological models, Tech. Rep. 22, EU WATCH (Water and global Change) project, 2010.

Weedon, G. P., Gomes, S., Viterbo, P., Shuttleworth, W. J., Blyth, E., Österle, H., Adam, J. C., Bellouin, N., Boucher, O., and Best, M.: Creation of the WATCH Forcing Data and Its Use to Assess Global and Regional Reference Crop Evaporation over Land during the Twentieth Century, J. Hydrometeorol., 12, 823–848, doi:10.1175/2011JHM1369.1, 2011.

Wilhite, D.: Drought: A global assessment, Routledge, London, 2000.

Wilson, D., Hisdal, H., and Lawrence, D.: Has streamflow changed in the Nordic countries? – Recent trends and comparisons to hydrological projections, J. Hydrol., 394, 334–346, doi:10.1016/j.jhydrol.2010.09.010, 2010.

Wong, W. K., Beldring, S., Engen-Skaugen, T., Haddeland, I., and Hisdal, H.: Climate Change Effects on Spatiotemporal Patterns of Hydroclimatological Summer Droughts in Norway, J. Hydrometeorol., 12, 1205–1220, doi:10.1175/2011JHM1357.1, 2011.

Yevjevich, V.: An objective approach to definition and investigation of continental hydrological droughts, Hydrology papers, 23, Colorado state university, Fort Collins, USA, 1967.